


# Characterization of cold atoms based on photoionization momentum spectra

Zhixian Wu(吴志贤), Shushu Ruan(阮舒舒), Zhenjie Shen(沈镇捷), Jie Liu(刘杰), Xinglong Yu(余兴龙), Lifeng Chen(陈利丰), Bing Zhu(朱兵), Xincheng Wang(王新成), and Yuhai Jiang(江玉海)

**Citation:**Chin. Phys. B, 2025, 34 (**7**): 073202. DOI: 10.1088/1674-1056/add00d
http://cpb.iphy.ac.cn; http://iopscience.iop.org/cpb

**What follows is a list of articles you may be interested in**

---

## Wavelength- and ellipticity-dependent photoelectron spectra from multiphoton ionization of atoms

Keyu Guo(郭珂雨), Min Li(黎敏), Jintai Liang(梁锦台), Chuanpeng Cao(曹传鹏), Yueming Zhou(周月明), and Peixiang Lu((陆培祥)

Chin. Phys. B, 2023, 32 (**2**): 023201. DOI: 10.1088/1674-1056/ac9b36

## Multiphoton quantum dynamics of many-electron atomic and molecular systems in intense laser fields

Peng-Cheng Li(李鹏程), Shih-I Chu

Chin. Phys. B, 2020, 29 (**8**): 083202. DOI: 10.1088/1674-1056/ab9c0f

## Comparative study on atomic ionization in bicircular laser fields by length and velocity gauges S-matrix theory

Hong Xia(夏宏), Xin-Yan Jia(贾欣燕), Xiao-Lei Hao(郝小雷), Li Guo(郭丽), Dai-He Fan(樊代和), Gen-Bai Chu(储根柏), Jing Chen(陈京)

Chin. Phys. B, 2020, 29 (**2**): 023204. DOI: 10.1088/1674-1056/ab610c

## Photoelectron imaging of resonance-enhanced multiphoton ionization and above-threshold ionization of ammonia molecules in a strong 800-nm laser pulse

Le-Le Song(宋乐乐), Ya-Nan Sun(孙亚楠), Yan-Hui Wang(王艳辉), Xiao-Chun Wang(王晓春), Lan-Hai He(赫兰海), Si-Zuo Luo(罗嗣佐), Wen-Hui Hu(胡文惠), Qiu-Nan Tong(佟秋男), Da-Jun Ding(丁大军), Fu-Chun Liu(刘福春)

Chin. Phys. B, 2019, 28 (**6**): 063201. DOI: 10.1088/1674-1056/28/6/063201

## Above-threshold ionization of hydrogen atom in chirped laser fields

Yuan-Yuan Ni(倪园园), Song-Feng Zhao(赵松峰), Xiao-Yong Li(李小勇), Guo-Li Wang(王国利), Xiao-Xin Zhou(周效信)

Chin. Phys. B, 2018, 27 (**7**): 073203. DOI: 10.1088/1674-1056/27/7/073203

---

**SPECIAL TOPIC — Ultrafast physics in atomic, molecular and optical systems**

# Characterization of cold atoms based on photoionization momentum spectra

Zhixian Wu(吴志贤)[1], Shushu Ruan(阮舒舒)[2], Zhenjie Shen(沈镇捷)[1,†], Jie Liu(刘杰)[2], Xinglong Yu(余兴龙)[2], Lifeng Chen(陈利丰)[1], Bing Zhu(朱兵)[3], Xincheng Wang(王新成)[1], and Yuhai Jiang(江玉海)[1,2,4,‡]

[1] *Center for Transformative Science and School of Physical Science and Technology, ShanghaiTech University, Shanghai* 201210, *China*
[2] *Shanghai Advanced Research Institute, Chinese Academy of Sciences, Shanghai* 201210, *China*
[3] *HSBC Laboratory, Guangzhou* 510510, *China*
[4] *School of Physics, Henan Normal University, Xinxiang* 453007, *China*

(Received 13 March 2025; revised manuscript received 18 April 2025; accepted manuscript online 24 April 2025)

We propose a method to characterize the features of a cold strontium cloud in a magneto-optical trap (MOT) through the photoionization of cold Sr atoms in a custom-designed reaction microscope. Sr atoms in the dark state of $5s5p\,^3P_2$ populated via the cascade transition $5s5p\,^1P_1 \rightarrow 5s4d\,^1D_2 \rightarrow 5s5p\,^3P_2$ accumulate a significant fraction, giving a long lifetime of 520 s. These atoms in the dark state are subsequently trapped by the gradient magnetic field of the MOT. By scanning the $Sr^+$ momentum distributions ionized with an 800 nm infrared femtosecond laser, we are able to outline the size of $\sim 0.55$ mm in radius and the temperature of $\sim 0.40$ mK for the dark-state atoms, which is significantly cooler than the MOT temperature of 3.3 mK trapped in the 461 nm. The size of MOT exhibits an oblate spheroidal distribution with a radius of approximately 0.35 mm and 0.55 mm, extracted with momenta of photoion and absorption imaging, respectively. The results using the photoion momenta are consistent with the expected results from absorption imaging, which confirms the method's reliability. The advantage of this method is the ability to simultaneously characterize the distribution information of atoms in different initial states within the cold atomic cloud.

**Keywords:** multiphoton ionization, photoelectron momentum, magneto-optical trap (MOT)

**PACS:** 32.80.Rm, 37.10.De

**DOI:** 10.1088/1674-1056/add00d **CSTR:** 32038.14.CPB.add00d

## 1. Introduction

The magneto-optical trap (MOT) is the main method of cooling and trapping atoms,[1,2] allowing the preparation of cold atomic samples with high densities. Cold-atom systems also play an important role in the fields of quantum computing, quantum simulation,[3–5] and precision measurement.[6–9] Nowadays, by applying MOT techniques to recoil ion momentum spectrometry or reaction microscopy, the recoil-ion momentum resolution can be significantly improved.[10–14] Such an experimental approach allows one to study ultrafast strong field ionization dynamics for alkali and alkaline-earth atoms, which has attracted increasing attention in the past few decades with the advent of a magneto-optical trap reaction microscope (MOTREMI).[15,16] Moreover, cold atoms can be effectively prepared and manipulated through the control of the magnetic quantum number $m$ with cooling lasers so that a complete measurement with full characterizations of initial- and final-state wave functions is accessible, exhibiting a benchmark one-photon single-ionization study of the hydrogen-like atom.[17]

Temperature and density are critical indicators for the profiles of a cold atomic cloud, by which Bose–Einstein condensation (BEC) of the atomic ensemble can be achieved.[18,19] These parameters also play an important role in the study of formation and evolution in ultra-cold plasmas.[20–22] The interactions of Rydberg atoms, photon recoil effects, and Autler–Townes,[23–25] etc. were studied with an ultra-cold strontium gas. The commonly used methods for measuring the temperature and density distribution of a cold atomic cloud include fluorescence imaging or absorption measurement,[13,26] the time-of-flight (TOF) technique,[27] and other methods. These methods require the use of laser light with corresponding wavelengths for imaging or probing, and temperature measurement typically involves turning off the cooling light to release the cold atomic cloud and interrupt the cooling cycle.

The present method based on photoionization provides a quantitative characterization of the spatial distribution of MOT and dark-state atoms, as well as the temperature of dark-state atoms, based on the differences in ion momentum distributions obtained from multiphoton single-ionization at different positions within the cold atomic cloud. The distribution of differ-

†Corresponding author. E-mail: shenzhj2@shanghaitech.edu.cn
‡Corresponding author. E-mail: jiangyh3@shanghaitech.edu.cn

© 2025 Chinese Physical Society and IOP Publishing Ltd. All rights, including for text and data mining, AI training, and similar technologies, are reserved.

ent atomic states can be obtained simultaneously by measuring variations in ion count at different positions within the cold atomic cloud.

The paper is organized as follows. In Section 2, we introduce the experimental setup and method. In Section 3, the size and temperature of the cold atomic cloud are calibrated using absorption imaging and photoionization methods, respectively. In Section 4, a summary of the present work and a brief outlook for our future investigations are provided.

## 2. Experimental setup and method

The present work is based on a home-made MOTREMI setup for cold strontium atoms.[15] Briefly, solid strontium is heated to 450 °C–550 °C in an oven to produce atomic vapor. These hot atoms are precooled and trapped under the influence of a Zeeman slower and a two-dimensional magneto-optical trap (2D MOT). The atoms in 2D MOT are pushed into the science chamber by a 461 nm CW laser beam to form a three-dimensional magneto-optical trap (3D MOT). The quadrupole magnetic field for the 3D MOT is provided by a pair of anti-Helmholtz coils, with a working current of 30 A and a magnetic field gradient of 32.4 G/cm.

The schematic diagram of the relevant transitions for the laser cooling of $^{88}$Sr is shown in Fig. 1. In this setup, the transition of $5s^2\,{}^1S_0 \rightarrow 5s5p\,{}^1P_1$ at 461 nm is adopted. Atoms in $5s5p\,{}^1P_1$ have a probability of 1:50000 decaying to the $5s4d\,{}^1D_2$ state,[28] from which they decay further to $5s5p\,{}^3P_{1,2}$ with a branching ratio of 2:1, where $5s5p\,{}^3P_2$ is a dark state, which has a lifetime of 520 s.[29]

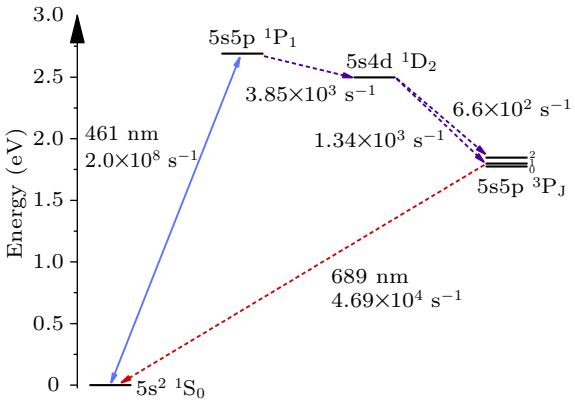



**Fig. 1.** The energy levels of strontium involved in the trapping of $^3P_2$ atoms. The decay rates (in units of $s^{-1}$) are provided. Laser light used for the experiment is indicated by blue solid lines.

Cold strontium atoms are ionized by a pulsed laser, and the generated recoil ions are accelerated by a weak uniform electric field ($\sim$ 1.7 V/cm). These charged fragments will be collected by a microchannel plate and a delay-line anode detector with $4\pi$ solid angle. By measuring the time of flight (TOF) and the hitting positions on the detector, the initial 3D momentum vectors of recoil ions can be reconstructed.

The size of the 3D MOT is obtained by using the absorption imaging method. The schematic diagram of the measurement is shown in Fig. 2. A few-μW imaging laser beam is coupled with one 3D cooling laser beam along the $z$-direction. A polarization beam splitter (PBS) is used to split the optical path, and a half-wave plate (HWP) is adjusted to maximize the reflection efficiency of the PBS without affecting the formation of the 3D MOT. A complementary metal oxide semiconductor (CMOS) camera is used for imaging.

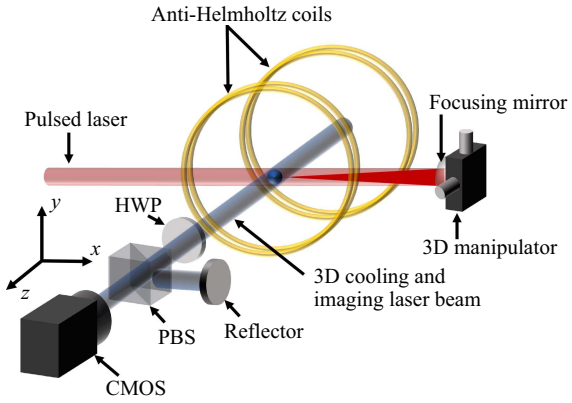



**Fig. 2.** The schematic diagram of measurement. Details of the operational processes are described in the text.

The imaging light is turned on to record the reference image without the 3D MOT. It is then turned off, while the cooling light and gradient magnetic field are activated to form the 3D MOT. The cooling light is turned off immediately and the imaging light is simultaneously turned on to capture the absorption image. By subtracting the background image from the absorption image, the 3D MOT image is obtained. Gaussian fitting is then applied to this image to determine the size of the 3D MOT.

The temperature of the 3D MOT is obtained by measuring its free expansion images of the atomic cloud using the absorption imaging method. Varying the free expansion time, a series of 3D MOT images is recorded. The standard deviations $\sigma_x$ and $\sigma_y$ are extracted with a two-dimensional Gaussian fitting on the atomic cloud images. The standard deviation of free expansion time $t$ is determined by

$$\sigma_{x,y}^2(t) = \sigma_0^2 + \frac{k_B T}{m} t^2, \tag{1}$$

where $\sigma_0$, $k_B$, $T$, $m$ are the standard deviation at the initial moment, the Boltzmann constant, the atomic cloud temperature, and the strontium atomic mass, respectively. With linear fitting, the temperature is determined by the slope.

By moving the 3D manipulator equipped with a focusing lens, as shown in Fig. 2, atoms at different positions within the cold atomic cloud are ionized. After scanning the laser focus along the radial direction of the magnetic field ($x$- and $y$-directions) to find the center of 3D MOT where the maximum ion yield is obtained, the laser focus is gradually moved along the axial direction of the magnetic field ($z$-direction),

meanwhile registering the variation of ion yield with position. The femtosecond laser used in the experiment has a central wavelength of 800 nm and a beam diameter of 5 mm before focusing. A lens with a focal length of 75 mm is employed to focus the beam. Based on Gaussian beam optics, the beam waist radius at the focus can be estimated by $\omega_0 = \lambda f/(\pi d)$, where $\lambda$ is the laser wavelength, $f$ is the focal length of the lens, and $d$ is the input beam diameter. Substituting the experimental parameters yields a waist radius of approximately 3.8 μm. To analyze the contribution of different initial states to ionization, we choose the light intensity of approximately 0.48 TW/cm$^2$. This intensity is significantly lower than the over-the-barrier ionization (OBI) threshold of strontium atoms, which is around 9 TW/cm$^2$.[30] The dominant ionization mechanism under our experimental conditions is multiphoton ionization (MPI).

## 3. Results and discussion

### 3.1. MOT size characterization based on absorption imaging and photoionization signals

According to the above method, figure 3 shows the measurement results of the absorption imaging. The radius of the atomic cloud in the 3D MOT in this plane is 0.55 mm by Gaussian fitting.

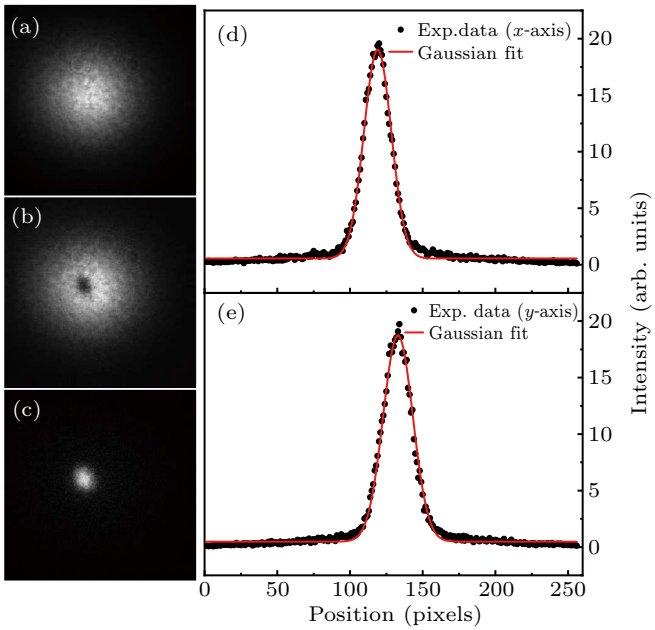



**Fig. 3.** Measurement of the atomic cloud size using the absorption imaging method. (a) Reference image, (b) absorption image, (c) atomic cloud distribution, (d) and (e) Gaussian fitting of the atomic cloud in two orthogonal directions ($x$-axis and $y$-axis). The black dots indicate the experimental data, while the red solid lines represent the Gaussian fit.

Figure 4 shows the relationship between the $Sr^+$ yield and the laser focus position in the $z$-direction, where the zero position corresponds to the maximum ion yield. The initial atomic states include $5s^2\,{}^1S_0$, $5s5p\,{}^1P_1$, $5s4d\,{}^1D_2$ and $5s5p\,{}^3P_2$, which require the absorption of 4, 2, 3, and 3 photons, respectively, for multi-photon single ionization. The relative probability $Y$ of ionization is sensitively dependent on $I$ by $Y \sim I^N$ ($N$ is the number of photons absorbed).[31] At a laser intensity of 3 TW/cm$^2$, the contributions of the single ionization of the $5s^2\,{}^1S_0$ and $5s5p\,{}^1P_1$ states are comparable.[16] For the laser intensity of 0.48 TW/cm$^2$ used in the experiment, according to $Y \sim I^N$, the contribution of $5s^2\,{}^1S_0$ is supposed to be at least one order of magnitude lower than that of $5s5p\,{}^1P_1$. Therefore, in the present work the contribution of $5s^2\,{}^1S_0$ to ionization is neglected. Based on our previous studies,[15,16] we have determined the momentum distributions of photoelectrons in the laser polarization direction that correspond to different ionization channels of the initial atomic states. For the $5s5p\,{}^1P_1$, the ionization channel $Sr(5s5p\,{}^1P_1) + 2\hbar\omega \rightarrow Sr^+ + e$, the magnitude of the electron momentum in the polarization direction of the pulsed laser is 0.03 a.u.; for the $5s4d\,{}^1D_2$, the ionization channel $Sr(5s4d\,{}^1D_2) + 3\hbar\omega \rightarrow Sr^+ + e$, the magnitude of the electron momentum in the polarization direction of the pulsed laser is 0.26 a.u.; and for the $5s5p\,{}^3P_2$, the ionization channels $Sr(5s5p\,{}^3P_2) + 3\hbar\omega \rightarrow Sr^+ + e$, the magnitude of the electron momentum in the polarization direction of the pulsed laser is 0.17 a.u.

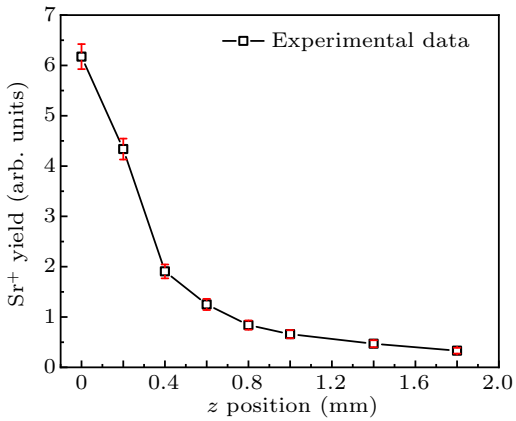



**Fig. 4.** The total yield of $Sr^+$ as a function of the laser focus position. The experimental data (black square) represents the measured $Sr^+$ yield at different laser focal positions.

Since momentum is conserved between the photoelectrons and $Sr^+$, the momentum distribution of the final-state ions in the laser polarization direction can be obtained by fitting these peaks, which allows us to determine the contribution of each initial state to the total ion yield. Figure 5 shows the momentum distributions of $Sr^+$ along the laser polarization direction at different positions, and the fitting curves are also shown in the figures. In the experiment, with fixed laser intensity, the ion yield is proportional to the initial atomic density. We used the ion yield obtained from the ionization of the $5s5p\,{}^1P_1$ state atoms at different positions to reflect the density distribution of the MOT. The positive axis of Fig. 6 shows the ion yield from the ionization of atoms of the state $5s5p\,{}^1P_1$ at different positions. By symmetrically extending the data from the positive half-axis of Fig. 6 to the negative half-axis and performing Gaussian fitting, we obtain the radius of the atomic cloud in this direction to be approximately 0.35 mm.

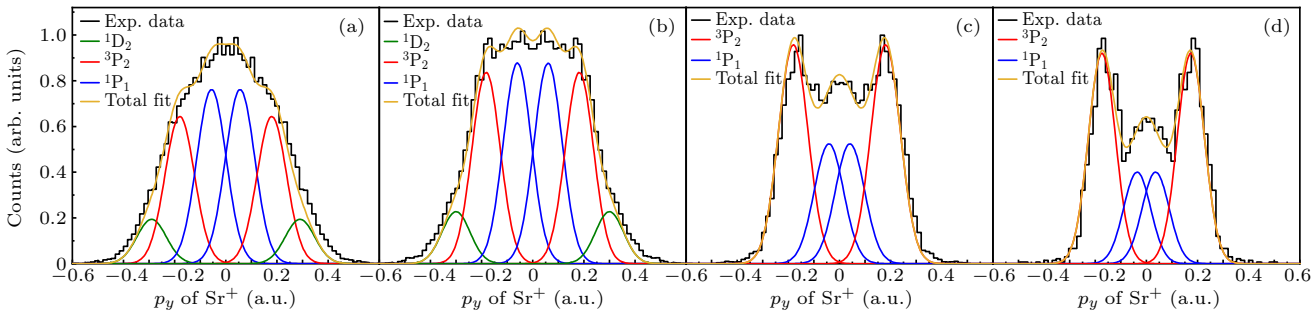



**Fig. 5.** Momentum distribution of $Sr^+$ along the laser polarization direction at 0 mm (a), 0.2 mm (b), 0.8 mm (c), and 1.4 mm (d), where the green, red, and blue lines represent the momentum peaks of 5s4d $^1D_2$, 5s5p $^3P_2$, and 5s5p $^1P_1$, respectively. The yellow line represents the result of multi-peak fitting. Note that distributions with $p_y < 0$ a.u. are mirrored from the positive parts.

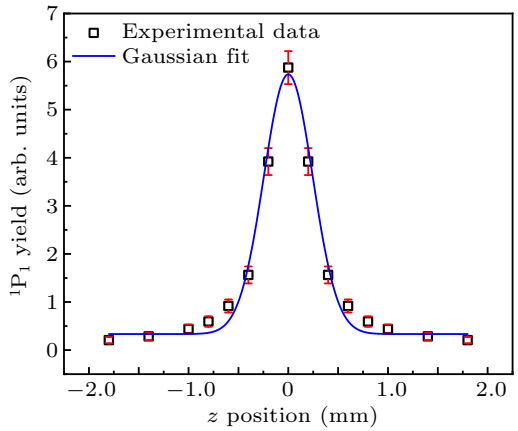



**Fig. 6.** Yield of 5s5p $^1P_1$ state atoms as a function of the laser focus position. The experimental data (black square) represents the measured yield of $Sr^+$ originating from the 5s5p $^1P_1$ state at different focal positions. The blue curve shows a Gaussian fit to the data. Note that distributions with $z < 0$ a.u. are mirrored from the positive parts.

This direction is along the axis of the anti-Helmholtz coil magnetic field, where the magnetic field gradient is twice that of the radial direction. According to the relationship between the MOT size and the magnetic field gradient, $\langle r \rangle \sim (\partial B/\partial r)^{-1/2}$,[32] the size of the atomic cloud along the $z$-axis is smaller than that obtained in the previous section using the absorption imaging method along the $x$- and $y$-directions.

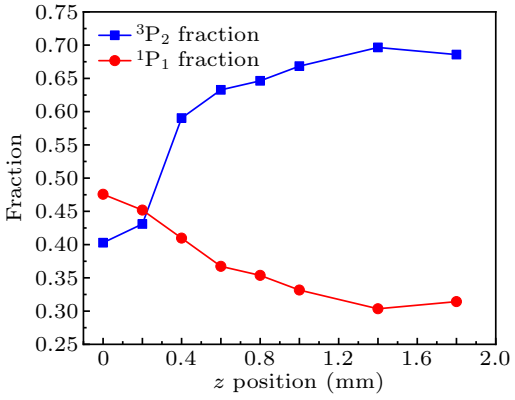



**Fig. 7.** Fraction of 5s5p $^3P_2$(blue squares) and 5s5p $^1P_1$(red circles) as a function of position.

As the laser scans towards the edge of the atomic cloud, the proportion of 5s5p $^3P_2$ atoms increases, while the population of 5s5p $^1P_1$ atoms decreases, as shown in Fig. 7. This observation indicates that the spatial distribution of dark-state atoms is broader than that of excited-state atoms.[33] By fitting the data in Fig. 8, the radius of dark-state atoms in the $z$-direction is approximately 0.55 mm, suggesting that the confinement effect of the magnetic trap is weaker than that of the magneto-optical trap.

### 3.2. Characterization of MOT and dark-state atom temperature

The temperature of the 3D MOT is obtained by measuring its free expansion images of the atomic cloud using the absorption imaging method. When the magnetic field gradient is 32.4 G/cm, the temperature is 3.3 mK. As shown in Fig. 1, the dark-state atoms in the MOT, which populate the long-lived 5s5p$^3P_2$ state through a cascade decay process, escape from the cooling cycle and no longer absorb photons from the 461 nm cooling light. Consequently, they do not experience the scattering force typically exerted on atoms undergoing repeated optical transitions. Instead, these atoms are solely influenced by the magnetic field gradient generated by the anti-Helmholtz coils, which provides a conservative trapping potential. This enables their confinement in a purely magnetic trap, distinct from the MOT mechanism. The magnetic field gradient force is a conservative force for atoms with a magnetic moment, and the spatial density distribution of atoms in the magnetic trap can be described by the Boltzmann distribution for a given potential field $U(r)$, and the atomic density $n(r)$ can be expressed as

$$n(r) = n_0 \exp\left(-\frac{U(r)}{k_B T}\right), \tag{2}$$

where $n_0$ is the atomic density at the center, $k_B$ is the Boltzmann constant, and $T$ is the temperature.

The potential energy of an atom with a magnetic dipole moment in a magnetic field is given by $U = -\boldsymbol{\mu} \cdot \boldsymbol{B}$, the projection of the magnetic dipole moment along the direction of the magnetic field is $\mu_z = -g_J \mu_B M_J$, $g_J$ is the Landé $g$-factor, $\mu_B$ is the Bohr magneton, and $M_J$ is the $z$ component of the quantum number of total angular momentum $J$. For 5s5p $^3P_2$, with $L = 1$, $S = 1$, and $J = 2$, the Landé $g$-factor is 1.5, as

derived from the following equation:

$$g_J = 1 + \frac{J(J+1)+S(S+1)-L(L+1)}{2J(J+1)}. \quad (3)$$

The corresponding $M_J$ values are $-2$, $-1$, 0, 1, 2. Only for atoms with $M_J > 0$, i.e., $M_J = 2$ or $M_J = 1$, the force experienced by the atoms points toward regions of weaker magnetic field and they are trapped in the magneto-optical trap.

By fitting the spatial distribution of the dark state using the Boltzmann distribution, we obtain the temperature information of the dark-state atoms. Figure 8 shows the ion yield from the ionization of the 5s5p $^3P_2$ state atoms at different positions. The solid blue line represents the Boltzmann distribution fit. In the fitting process, only the case of $M_J = 2$ is considered because the trapping efficiency of $M_J = 1$ is significantly reduced. This reduction occurs because these atoms are more likely to be lost due to spin-exchange collisions[34] and the $M_J = 2$ state has a larger magnetic moment, resulting in a higher trapping efficiency in the MOT. Through fitting, the temperature of the dark-state atoms is determined to be $\sim 0.40$ mK, which is about an order of magnitude lower than that of the 3D MOT. It indicates that evaporative cooling occurs during the formation of the magnetic trap.[35] Atoms with a temperature higher than the depth of the magnetic trap will escape the trap, leaving behind lower temperature atoms, which reduces the overall temperature of the 5s5p $^3P_2$ atomic cloud.

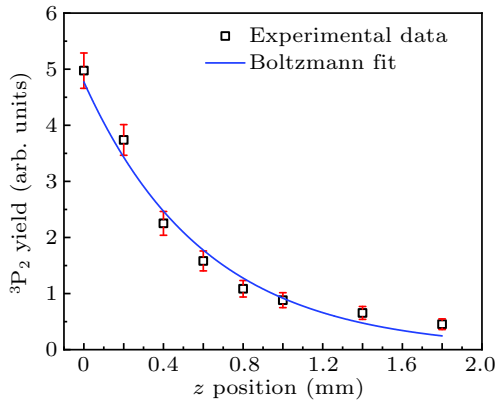



**Fig. 8.** Yield of 5s5p $^3P_2$ state atoms as a function of the laser focus position. The experimental data (black square) represents the measured yield of $Sr^+$ originating from the 5s5p $^3P_2$ state at different focal positions. The blue curve represents the Boltzmann distribution fitting.

## 4. Conclusion

This study investigates the dark-state distribution of strontium atoms and the temperature characteristics of dark-state atoms in MOT using femtosecond laser ionization momentum imaging techniques. The atomic distribution in the MOT was characterized using absorption imaging and photoionization techniques, revealing the impact of the magnetic-field gradient on the MOT size. The temperature information of the dark-state atoms in the MOT was obtained, and it was confirmed that evaporative cooling occurred during the confinement of the dark-state atoms, providing a new perspective for the study of cold atomic systems. This method can simultaneously extract information on atoms in different states within the cold atomic cloud, facilitating the study of cold atomic dynamics in complex external fields.

## Acknowledgements

Project supported by the Natural Science Foundation of Henan (Grant No. 252300421304), the National Natural Science Foundation of China (Grant Nos. 12204498, 12474259, and 12334011), and the National Key Research and Development Program of China (Grant No. 2022YFA1604302). The authors also acknowledge the computational resource of the HPC platform in ShanghaiTech University.

## References

[1] Raab E L, Prentiss M, Cable A, Chu S and Pritchard D E 1987 *Phys. Rev. Lett.* **59** 2631
[2] Tan Z, Lu B, Han C and Lee C 2024 *Chin. Phys. B* **33** 093701
[3] Gross C and Bloch I 2017 *Science* **357** 995
[4] Bloch I, Dalibard J and Zwerger W 2008 *Rev. Mod. Phys.* **80** 885
[5] Bloch I, Dalibard J and Nascimbène S 2012 *Nat. Phys.* **8** 267
[6] Bothwell T, Kedar D, Oelker E, Robinson J M, Bromley S L, Tew W L, Ye J and Kennedy C J 2019 *Metrologia* **56** 065004
[7] Ludlow A D, Boyd M M, Ye J, Peik E and Schmidt P O 2014 *Rev. Mod. Phys.* **87** 637
[8] Schioppo M, Brown R C, McGrew W F, Hinkley N, Fasano R J, Beloy K, Yoon T H, Milani G, Nicolodi D, Sherman J A, Phillips N B, Oates C W and Ludlow A D 2017 *Nat. Photon.* **11** 48
[9] Zheng X, Dolde J, Lochab V, Merriman B N, Li H and Kolkowitz S 2022 *Nature* **602** 425
[10] Li R, Yuan J, Wang X, Hou X, Zhang S, Zhu Z, Ma Y, Gao Q, Wang Z, Yan T, Qin C, Li S, Zhang Y, Weidemüller M and Jiang Y 2019 *JINST* **14** 02022
[11] Yuan J, Ma Y, Li R, Ma H, Zhang Y, Ye D, Shen Z, Yan T, Wang X, Weidemüller M and Jiang Y 2020 *Chin. Phys. Lett.* **37** 053201
[12] Yuan J, Liu S, Wang X, Shen Z, Ma Y, Ma H, Meng Q, Yan T M, Zhang Y, Dorn A, Weidemüller M, Ye D and Jiang Y 2020 *Phys. Rev. A* **102** 043112
[13] Ma Y, Li R, Yuan J, Meng Q, Ma H, Ruan S, Zhang Y, Yan T, Shen Z, Wang X and Jiang Y 2020 *Chinese Journal of Lasers* **47** 0601011 (in Chinese)
[14] Ma H, Wang X, Zhang L, Zou Z, Yuan J, Ma Y, Lv R, Shen Z, Yan T, Weidemüller M, Ye D and Jiang Y 2023 *Phys. Rev. A* **107** 033114
[15] Ruan S, Yu X, Shen Z, Wang X, Liu J, Wu Z, Tan C, Chen P, Yan T M, Ren X, Weidemüller M, Zhu B and Jiang Y 2024 *Phys. Rev. A* **109** 023118
[16] Ruan S, Han Y, Shen Z, Yu X, Fang Y K, Wang X, Chen A, Liu J, Wu Z, Ueda K, Weidemüller M, Zhu B, Peng L Y and Jiang Y 2024 *Phys. Rev. A* **110** 033114
[17] Ma H, Zhang L, Wang X, Zou Z, Lv R, Shen Z, Chen A, Weidemüller M, Ueda K, Ye D and Jiang Y 2025 *Phys. Rev. Lett.* **134** 123204
[18] Anderson M, Ensher J, Matthews M, Wieman C and Cornell E 1995 *Science* **269** 198
[19] Cornell E A and Wieman C E 2002 *Rev. Mod. Phys.* **74** 875
[20] Killian T C, Kulin S, Bergeson S D, Orozco L A, Orzel C and Rolston S L 1999 *Phy. Rev. Lett.* **83** 4776
[21] Killian T C, Chen Y C, Gupta P, Laha S, Martinez Y N, Mickelson P G, Nagel S B, Saenz A D and Simien C E 2005 *J. Phys. B: Atom. Mol. Opt. Phys.* **38** S351

[22] Bergeson S D, Baalrud S D, Ellison C L, Grant E, Graziani F R, Killian T C, Murillo M S, Roberts J L and Stanton L G 2019 *Phys. Plasmas* **26** 100501
[23] Qiao C, Tan C, Siegl J, Hu F, Niu Z, Jiang Y, Weidemüller M and Zhu B 2021 *Phys. Rev. A* **103** 063313
[24] Tan C, Hu F, Niu Z, Jiang Y, Weidemüller M and Zhu B 2022 *Chin. Phys. Lett.* **39** 093202
[25] Hu F, Tan C, Jiang Y, Weidemüller M and Zhu B 2022 *Chin. Phys. B* **31** 016702
[26] Chu S, Hollberg L, Bjorkholm J E, Cable A and Ashkin A 1985 *Phys. Rev. Lett.* **55** 48
[27] Lett P D, Watts R N, Westbrook C I, Phillips W D, Gould P L and Metcalf H J 1988 *Phys. Rev. Lett.* **61** 169
[28] Xu X, Loftus T H, Hall J L, Gallagher A and Ye J 2003 *J. Opt. Soc. Am. B* **20** 968
[29] Yasuda M and Katori H 2004 *Phys. Rev. Lett.* **92** 153004
[30] Dimitriou A, Loriot V, Marciniak A, Barillot T, Danakas S, Lépine F, Bordas C and Cohen S 2022 *Phys. Rev. A* **105** 053106
[31] Fabre F, Petite G, Agostini P and Clement M 1982 *J. Phys. B: Atom. Mol. Opt. Phys.* **15** 1353
[32] Petrich W, Anderson M H, Ensher J R and Cornell E A 1994 *J. Opt. Soc. Am. B* **11** 1332
[33] Hu F, Nosske I, Couturier L, Tan C, Qiao C, Chen P, Jiang Y H, Zhu B and Weidemüller M 2019 *Phys. Rev. A* **99** 033422
[34] Kokkelmans S J J M F, Boesten H M J M and Verhaar B J 1997 *Phys. Rev. A* **55** R1589
[35] Nagel S B, Simien C E, Laha S, Gupta P, Ashoka V S and Killian T C 2003 *Phys. Rev. A* **67** 011401